

Study of $B^+ \rightarrow D_s^{(*)+} \pi^0$ mode at Belle

Manish Kumar^{a,*} and Vishal Bhardwaj^a

(On behalf of Belle II collaboration)

^aIndian Institute of Science Education and Research Mohali,
Knowledge city, Sector 81, SAS Nagar, Manauli, India

E-mail: manishkumar@iisermohali.ac.in, vishal@iisermohali.ac.in

We present here the sensitivity study of the rare decay modes $B^+ \rightarrow D_s^+ \pi^0$ and $B^+ \rightarrow D_s^{(*)+} \pi^0$, at Belle using a simulated sample. The BABAR collaboration has measured the branching fraction $\mathcal{B}(B^+ \rightarrow D_s^+ \pi^0) = (1.5_{-0.4}^{+0.5} \pm 0.1 \pm 0.2) \times 10^{-5}$ with a data sample of $232 \times 10^6 B\bar{B}$ events collected at the $\Upsilon(4S)$ resonance. The combined data from the Belle and Belle II experiments is five times larger than the previously used. This will allow us to provide an improved measurement of the branching fraction for these decay modes, for a better bound on the ratio of the amplitudes $r_{D\pi} = \frac{A(B^0 \rightarrow D^+ \pi^-)}{A(B^0 \rightarrow D^- \pi^+)}$ (assuming SU(3) symmetry), which is important input to extract weak phases in the time-dependent measurement of $B^0 \rightarrow D^\pm \pi^\mp$ decays.

In addition, we aim to search for the $B^+ \rightarrow D_s^{(*)+} \pi^0$ mode, whose upper limit is provided by the ARGUS collaboration based on $209 \times 10^3 B\bar{B}$ events.

16th International Conference on Heavy Quarks and Leptons (HQL2023)
28 November-2 December 2023
TIFR, Mumbai, Maharashtra, India

*Speaker

1. Introduction

The rare decay $B^+ \rightarrow D_s^{(*)+} \pi^0$ is expected to be dominated by the spectator diagram as shown in fig. 1, which is suppressed by the Cabibbo-Kobayashi-Maskawa factor $|V_{ub}| \sim \lambda^3$ [1]. Improved measurement of the branching fraction for this rare decay mode helps in a better bound on the ratio of the amplitudes, $r_{D\pi} \rightarrow A(B^0 \rightarrow D^+ \pi^-)/A(B^0 \rightarrow D^- \pi^+)$, which is an important input to extract the weak phase $(2\phi_1 + \phi_3)$ in the time-dependent measurement of $B^0 \rightarrow D^\pm \pi^\mp$ mode.

The BABAR collaboration has determined the branching fraction $B^+ \rightarrow D_s^+ \pi^0$ mode using the

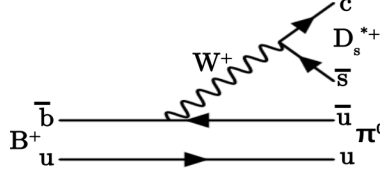


Figure 1: Feynman diagram for $B^+ \rightarrow D_s^{(*)+} \pi^0$ mode.

sample of $232 \times 10^6 B\bar{B}$ [2] events gathered at the $\Upsilon(4S)$ resonance. In addition, the upper limit on the branching fraction of $B^+ \rightarrow D_s^{(*)+} \pi^0$ decay mode was set at the 90% confidence level by the ARGUS collaboration based on the sample of $209 \times 10^3 B\bar{B}$ [3] events. Comparatively, the combined data set from the Belle and Belle II experiments exceeds the BABAR (ARGUS) data size by approximately five (five thousand) times for analyzing the $B^+ \rightarrow D_s^+ \pi^0$ ($B^+ \rightarrow D_s^{(*)+} \pi^0$) decay mode. In this proceeding, we present the study of $B^+ \rightarrow D_s^+ \pi^0$ and $B^+ \rightarrow D_s^{(*)+} \pi^0$ modes, using a simulated sample from the Belle experiment.

2. Analysis Strategy

For this study, we plan to use the combined data of the Belle [4] and Belle II [5] experiment which is collected by the asymmetric collision of electron and positron at the $\Upsilon(4S)$ resonance. Here, we present the study using the simulated Belle sample. To validate the analysis procedure, determine efficiencies, and study backgrounds, we use samples of simulated data generated with EvtGen [6] with QED final-state radiation generated by PHOTOS [7]. The detector response is incorporated using GEANT 3 [8]. For background studies, we use three separate simulation samples that include $e^+e^- \rightarrow B\bar{B}$ and $q\bar{q}$ ($q = u, d, s, c$) events. We perform the analysis using the B2BII software package [9], which converts Belle data into a format compatible with the Belle II software framework [10].

We select tracks consistent with originating from the interaction point by requiring $d_r < 0.5$ and $|d_z| < 4.0$ cm, where d_r and d_z are the track impact parameters in the plane transverse and parallel to the beam axis, respectively. We require $\pi^0 \rightarrow \gamma\gamma$ candidates to have an invariant mass $M_{\gamma\gamma}$ within the range $[0.11, 0.16]$ GeV/c^2 , which corresponds to $\pm 3\sigma$ about the nominal mass of the π^0 meson [11], with σ being the mass resolution. To avoid the background from the low momentum π^0 candidates, we select π^0 having the center-of-momentum greater than $2.1 \text{ GeV}/c$. We retain only the ϕ , \bar{K}^{*0} , and K_S^0 candidates having invariant masses within 14, 100, and 10 MeV/c^2 of their known values [11].

The invariant masses of D_s^+ reconstructed from the $\phi\pi^+$, $\bar{K}^{*0}K^+$, $K_S^0K^+$ are required to be within $\pm 3\sigma$ of the nominal mass D_s^+ mesons [11]. For the reconstruction of B candidates we utilize two kinematic variables: the energy difference $\Delta E = E_B - E_{\text{beam}}$, where E_{beam} is the beam energy and E_B is the B -candidate energy, both calculated in the center-of-mass (c.m.) frame; and the beam-constrained mass $M_{\text{bc}} = \sqrt{(E_{\text{beam}}/c^2)^2 - (\vec{p}_B/c)^2}$, where \vec{p}_B is the momentum of the B meson candidate in the c.m. frame.

The production cross section of $e^+e^- \rightarrow q\bar{q}$ is approximately 3 times that of $B\bar{B}$ production at energies close to the $\Upsilon(4S)$ resonance, making the continuum background suppression necessary in all modes of interest. In the c.m. frame, continuum events generally have particles collimated into back-to-back jets, whereas the particles from the nearly-at-rest B mesons produced in $B\bar{B}$ events are isotropically distributed over the full solid angle. Therefore, we combine event-shape variables and flavor-tagging information using a multivariate classifier FastBDT [12] to distinguish between continuum and $B\bar{B}$ events. We require candidates to have FastBDT classifier output (C) > 0.96; this criterion is optimized by maximizing the figure of merit defined in Ref. [13] and retains 39% of signal events, while removing approximately 99% of background events, for $B^+ \rightarrow D_s^+\pi^0$ decay mode as shown in fig 2 with and without C. The signal yield is extracted from the 2D unbinned maximum-

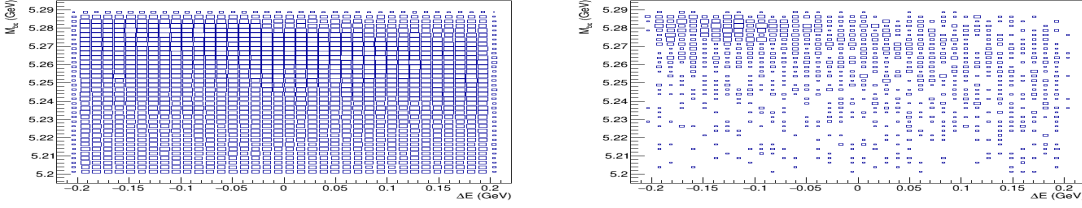


Figure 2: M_{bc} versus ΔE distribution without C (left) and with $C > 0.96$ (right) for $B^+ \rightarrow D_s^+\pi^0$ mode.

likelihood fitted between the ΔE and M_{bc} distributions as shown in fig. 3. The signal yield are

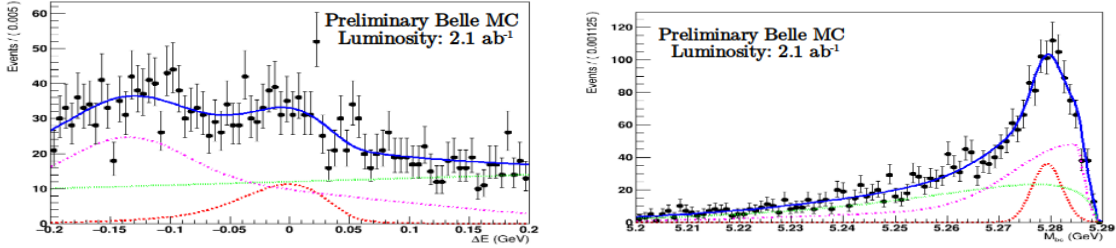


Figure 3: 2D UML fitted distribution of the ΔE and M_{bc} with simulation for $B^+ \rightarrow D_s^+\pi^0$ decay mode. The different curves such as the solid blue, dotted red, magenta, green line for the total, signal (expected from the luminosity), peaking, and combinatorial background PDFs, respectively.

expected from the luminosity and generated from the ToyMC study. For $B^+ \rightarrow D_s^+\pi^0$ decay modes, the signal probability density function (PDF) shape in the ΔE and M_{bc} distribution is parameterized with the sum of a logarithmic Gaussian and Gaussian function with a common mean and sum of two Gaussians with a common mean, respectively. In $B^+ \rightarrow D_s^+\pi^0$, the peaking background at $\Delta E \sim -0.15$ GeV comprises candidates reconstructed from $B^0 \rightarrow D^-\rho^+$ and $B^+ \rightarrow D^0\rho^+$ decay

modes. The peaking background from partially reconstructed B decays is modeled using a sum of two Gaussian functions with a common mean and sum of two bifurcated Gaussian functions with a common mean for ΔE and M_{bc} , respectively. The combinatorial background, mainly from continuum events, is modeled with a straight line and Argus function for ΔE and M_{bc} distribution, respectively.

3. Summary

In summary, we demonstrate the feasibility of studying $B^+ \rightarrow D_s^+ \pi^0$ decay mode using the Belle simulation samples. We have optimized the selection criteria for discrimination of the signal and background events. The main continuum background source is suppressed, by using FastBDT method. Finally, for the extraction of signal yield, we used 2D UML fitted distribution of ΔE and M_{bc} variable. Here, we shown the distribution with the Belle simulated sample. We plan to do the simulation study for signal modes with the Belle II simulation sample and once we have understood both detectors we will look at the data.

References

- [1] N. Cabibbo, Phys. Rev. Lett. **10**, 531 (1963); M. Kobayashi and T. Maskawa, Prog. Theor. Phys. **49**, 652 (1973).
- [2] B. Aubert *et al.* (BABAR Collaboration), Phys. Rev. Lett. **98**, 171801 (2007).
- [3] H. Albrecht *et al.* (ARGUS Collaboration), Z. Phys. C. **60**, 11-18 (1993).
- [4] A. Abashian *et al.* (Belle Collaboration), Nucl. Instrum. Methods Phys. Res. Sect. A **479**, 117 (2002); also see detector section in J. Brodzicka *et al.*, Prog. Theor. Exp. Phys. **2012**, 04D001 (2012).
- [5] E. Kou *et al.*, The Belle II Physics Book, **2019**, 123C01 (2019).
- [6] D.J. Lange, Nucl. Instrum. Methods Phys. Res. Sect. A **462**, 152 (2001).
- [7] E. Barberio and Z. Was, Comput. Phys. Commun. **79**, 291 (1994).
- [8] R. Brun *et al.*, GEANT 3.21, CERN Program Library Long Writeup W5013, unpublished.
- [9] M. Gelb *et al.*, B2BII: Data Conversion from Belle to Belle II, arXiv:1810.00019.
- [10] T. Kuhr *et al.* (Belle II Framework Software Group), Comput. Softw. Big Sci. **3**, 1 (2019).
- [11] P. A. Zyla *et al.* (Particle Data Group), Prog. Theor. Exp. Phys. 2020, 083C01 (2020), and 2021 update.
- [12] T. Keck, Computing and Software for Big Science **1**, 2 (2017), <https://doi.org/10.1007/s41781-017-0002-8>.
- [13] G. Punzi, Sensitivity of searches for new signals and its optimization, arXiv:physics/0308063v2.